Cell Tissue Res (2006) 323: 465–474
DOI 10.1007/s00441-005-0100-5

REGULAR ARTICLE

D. F. Egging · I. van Vlijmen · B. Starcher · Y. Gijsen · M. C. Zweers · L. Blankevoort · J. Bristow · J. Schalkwijk

Dermal connective tissue development in mice: an essential role for tenascin-X

Received: 28 September 2005 / Accepted: 10 October 2005 / Published online: 6 December 2005

Abstract Deficiency of the extracellular matrix protein tenascin-X (TNX) causes a recessive form of Ehlers–Danlos syndrome (EDS) characterized by hyperextensible skin and hypermobile joints. It is not known whether the observed alterations of dermal collagen fibrils and elastic fibers in these patients are caused by disturbed assembly and deposition or by altered stability and turnover. We used biophysical measurements and immunofluorescence to study connective tissue properties in TNX knockout and wild-type mice. We found that TNX knockout mice, even at a young age, have greatly disturbed biomechanical properties of the skin. No joint abnormalities were noted at any age. The spatio-temporal expression of TNX during normal mouse skin development, during embryonic days 13–19 (E13–E19), was distinct from tropoelastin and the dermal fibrillar collagens type I, III, and V. Our data show that TNX is not involved in the earliest phase (E10–E14) of the deposition of collagen fibrils and elastic fibers during fetal development. From E15 to E19, TNX starts partially to colocalize with the dermal collagens and elastin, and in adult mice, TNX is present in the entire dermis. In adult TNX knockout mice, we observed an apparent increase of elastin. We conclude that TNX knockout mice only partially recapitulate the phenotype of TNX-deficient EDS patients, and that TNX could potentially be involved in maturation and/or maintenance of the dermal collagen and elastin network.

Keywords Tenascin-X · Collagen · Elastin · Development · Ehlers-Danlos syndrome · Mouse (TNX knockout)

D. F. Egging (✉) · I. van Vlijmen · M. C. Zweers · J. Schalkwijk
Department of Dermatology Nijmegen,
Centre for Molecular Life Sciences,
Radboud University Nijmegen Medical Centre,
P.O. Box 9101, 6500 HB Nijmegen, The Netherlands
e-mail: d.egging@derma.umcn.nl

B. Starcher
Department of Biochemistry,
University of Texas Health Center at Tyler,
Tyler, TX, USA

Y. Gijsen · L. Blankevoort
Department of Orthopedics,
Orthotrauma Research Center Amsterdam,
Academic Medical Center,
University of Amsterdam,
Amsterdam, The Netherlands

J. Bristow
Department of Pediatrics, University of California,
San Francisco, CA, USA

J. Bristow
Department of Genome Sciences,
Lawrence Berkeley National Laboratory,
Berkeley, CA, USA

Introduction

TNX is a large extracellular matrix glycoprotein (Bristow et al. 1993; Lethias et al. 1996; Elefteriou et al. 1997; Ikuta et al. 1998) that is expressed in a variety of tissues including skin, joints, heart, and blood vessels. Complete deficiency of TNX in humans leads to a recessive form of Ehlers-Danlos syndrome (EDS), and TNX haploinsufficiency is a cause of hypermobility type EDS (Burch et al. 1997; Schalkwijk et al. 2001; Zweers et al. 2003). Adult TNX-deficient patients show abnormal elastic fibers and reduced collagen deposition in skin (Zweers et al. 2004). We have recently found that a high serum TNX concentration is a risk indicator for abdominal aorta aneurysm (Zweers et al. 2005). TNX-deficient patients appear to have normal vessel wall compliance and distensibility of the large arteries; however, two out of nine described patients underwent surgery for mitral valve replacement (Peeters et al. 2004; Lindor and Bristow 2005).

Two groups have independently generated TNX knockout mice (Matsumoto et al. 2001; Mao et al. 2002). Mao et al. (2002) have shown that TNX knockout mice mimic EDS

through alterations in collagen deposition, as seen in TNX-deficient patients. Matsumoto et al. (2004a–c) have demonstrated altered fatty acid composition in TNX knockout mice compared with wild-type mice and increased MMP2 activation. The same group have found that tumour invasion and metastasis are enhanced in TNX knockout mice (Matsumoto et al. 2001, 2002). The enhanced tumor invasion found in TNX knockout mice is supported by the data on cutaneous malignant melanoma in MeLiM swine. These melanoma cells show a dramatic downregulation of TNX, which could account in part for the invasive phenotype of this tumor (Geffrotin et al. 2000).

In our previous study of the dermal abnormalities of five adult TNX index patients (Schalkwijk et al. 2001), we could not determine whether these alterations were attributable to developmental defects in the collagen and elastic fibre network, or to post-natal instability or breakdown. Here, we have investigated TNX expression in wild-type and TNX knockout mice during fetal skin development in relation to the expression of fibrillar collagens type I, III, and V and elastin. Our results indicate that the TNX knockout mouse is a suitable model for skin fragility but not for joint hypermobility. The reduced biomechanical strength of the skin in adult TNX knockout mice can be found in juvenile mice but is unlikely to be caused in the initial phase of deposition of the collagenous and elastic fibre network.

Materials and methods

Test animals

TNX knockout mice were obtained as described previously (Mao et al. 2002). For all studies, except for measurements of the medial collateral ligament (MCL), we used +/+, +/–, and –/– offspring from heterozygous parents obtained by the backcrossing of TNX knockout mice with four generations of C57/BL6 mice. For optical coherence tomography and measurements of the stiffness of the MCL, littermates (3–6 months old) were used from TNX heterozygous parents obtained by backcrossing with two generations of C57/BL6 mice. The number of mice for each test is indicated in the results. The experimental design was approved by the animal use committee of Radboud University, Nijmegen.

Processing of samples

At each time point, adult mice were killed in a sealed compartment by exposure to a mixture of carbogen gas and increasing concentrations of CO_2. Mouse fetuses were killed by decapitation. Complete hind legs of mice were stored at –20°C prior to measurements of the MCL and were processed as previously described (Gijssen et al. 2004). Skin samples for paraffin sections were fixed in buffered formalin for 4 h. Skin samples for frozen sections were embedded in Tissue–Tek O.C.T. compound (Sakura Finetek Europe, The Netherlands) and snap-frozen in liquid nitrogen. The breaking strength of mouse skin samples was measured immediately after the animals had been killed.

Histochemistry and immunohistochemistry

Staining of elastic fibers was performed by a modified Hart's method on paraffin sections (7 μm thick; Starcher et al. 2005). Paraffin and frozen sections (7 μm thick) were stained with antibodies against TNX, tropoelastin (TE), and collagens type I, III, and V. Detection was performed with antibodies conjugated to fluorescein isothiocyanate (FITC, green) and Alexa Fluor 594 (AF594, red; Table 1). Cell nuclei were counterstained with 4,6-diamidino-2-phenylindole (DAPI; Molecular Probes, The Netherlands; blue).

Computational analysis of (tropo) elastin and elastic fiber density

Each micrograph was analyzed by using IPlab software (Scanalytics, US). Once a representative "region of interest" (ROI), excluding hair follicles, had been chosen, all positive segments in the ROI were marked with a specific color. The surface of the colored area was divided by the ROI surface to determine the signal density.

Measurement of the stiffness of the MCL

The stiffness of the MCL was determined as previously described (Gijssen et al. 2004). Briefly, the tibia and femur of the mouse leg were clamped in a tensile tester. All tissues were removed from the femur and tibia with the exception of the MCL. Forces were applied in the longitudinal direction of the tibia and MCL.

Measurement of the cross-sectional area of the MCL by optical coherence tomography

Optical coherence tomography, which is the optical equivalent of ultasound imaging, is a noninvasive cross-sectional imaging technique for biological systems (Huang et al. 1991). For the imaging of the MCL, a reference point was visually determined at approximately the midpoint of the ligament, in between the tibia and femoral insertion (approximately 1 mm distal to the joint cavity). Images were taken from 2 mm distal to 2 mm proximal to the reference point to cover the full length of the MCL (approximately 3.5 mm). Cross-sectional images (β-scans) were made at 0.2-mm intervals to obtain a series of 21 β-scans along the full length of the ligament. The cross-sectional area of a MCL was calculated with custom analysis software written in Labview 7 (National Instruments, US) by using β-scans 8–15 in which the MCL was clearly visible and of constant dimensions. Optical coherence tomography has been previously validated for ligaments and tendons (Martin et al. 2003).

Table 1 Antibodies used for immunofluorescence studies

ECM constituents	Primary antibody mixture	Secondary antibody mixture
Elastin and TNX	Goat polyclonal anti-rat (tropo)elastin[a]	Chick polyclonal anti-goat AF594[f]
	Guinea pig anti-human TNX[b]	Rabbit polyclonal anti-guinea pig FITC[g]
Collagens type I and TNX	Goat polyclonal anti-human collagen I[c]	Chick polyclonal anti-goat AF594[f]
	Guinea pig anti-human TNX[b]	Rabbit polyclonal anti-guinea pig FITC[g]
Collagen type III and TNX	Goat polyclonal anti-human collagen III[d]	Chick polyclonal anti-goat AF594[f]
	Guinea pig anti-human TNX[b]	Rabbit polyclonal anti-guinea pig FITC[g]
Collagen type V and TNX	Goat polyclonal anti-human collagen V[e]	Chick polyclonal anti-goat AF594[f]
	Guinea pig anti-human TNX[b]	Rabbit polyclonal anti-guinea pig FITC[g]

[a]Elastin Products, USA
[b]Schalkwijk et al. 2001
[c]SouthernBiotech, USA
[d]SouthernBiotech, USA
[e]SouthernBiotech, USA
[f]Molecular Probes, The Netherlands
[g]Dakocytomation, Denmark

Flexibility of the tail

Increased flexibility of tail ligaments and tendons, as described for the TSP2-null mouse (Kyriakides et al. 1998), was ascertained for the TNX knockout mouse. In a blind randomized test, the animals were maintained under anesthesia at an isofluran dose of 2.5%–3.0% in a N_2O_2 gas mixture (50%–65% O_2) while the investigator attempted to tie a knot in the mouse tail.

Breaking strength

A rectangular strip of dorsal skin (7 mm × 3.5 cm) was prepared from the killed mice by using a custom-made apparatus. The skin segment was clamped in a device that exerted a continuously increasing force in a longitudinal direction. The breaking strength was defined as the peak force necessary to induce tearing of a tissue segment and was expressed in grams (1000 g is equivalent to 9.281 N), as described previously (Waard de et al. 1995).

Biochemical analysis of hydroxyproline and desmosine content

Desmosine analysis of mouse skin samples was used to measure the elastin content of the skin. After removal of the hair, a 3-mm biopsy punch was obtained from the caudal dorsal skin of the mice and placed in a secure-lock microfuge tube. The sample was hydrolyzed in 500 µl 6 N HCl at 105°C for 24 h. The hydrolysate was evaporated to dryness, re-dissolved in 200 µl water, and microfuged to remove insoluble material. A 20-µl aliquot was removed for desmosine analysis by radioimmunoassay (Starcher and Conrad 1995), and 1 µl was used for protein determination by a ninhydrin-based assay as described previously (Starcher 2001). Hydroxyproline (OHP) analysis was used as a method for measuring the collagen content of the skin. The OHP content was determined by amino acid analysis from the same hydrolysate as the desmosine analysis.

Results

Biomechanical properties of skin and joints in TNX knockout and wild-type mice

Littermates –/–, –/+, and +/+ for TNX were used to measure skin and joint biomechanical properties. Figure 1 shows the applied force required for skin failure (breaking strength). The breaking strength of TNX knockout mouse skin was significantly lower than that of heterozygous or wild-type littermates. The phenotype was appreciable even at the earliest possible age that could be investigated (2 weeks neonatal), and the difference in skin strength between wild-type and TNX knockout mice increased with age (Fig. 1). Wild-type and heterozygous mice did not significantly differ. To investigate joint laxity in these animals, we performed two tests. First, we tested whether

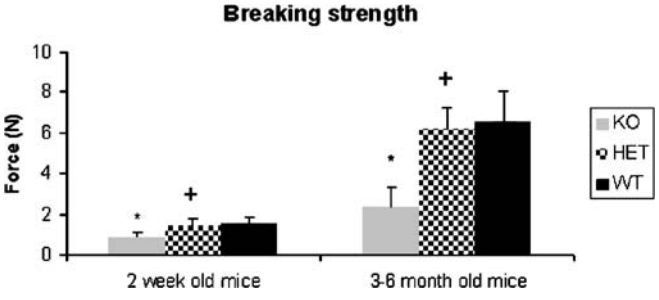

Fig. 1 Breaking strength of mouse skin. TNX knockout mice (*KO*) have weaker skin compared with that of heterozygous (*HET*) and wild-type (*WT*) littermates. The difference is appreciable even at a young age and increases over time (for comparisons of adult mice of 3–6 months of age, n=12 for knockout, n=6 for heterozygous, and n=5 for wild-type mice; for mice of 2 weeks of age, n=6 for knockout, n=8 for heterozygous, and n=10 for wild-type mice). For all comparisons to wild-type mouse, *P<0.001 when compared with knockout mice (+ not significant when compared with heterozygous mice)

Table 2 Biomechanical properties of the MCL of TNX knockout and wild-type littermates. The MCL of TNX knockout and wild-type littermates were the same in thickness and stiffness (for all comparisons, + not significant)

Character	Genotype	Mean	SD	*n*
Stiffness of MCL (N/mm)	Wild-type	5.08^{+}	1.12	8
	TNX knockout	4.96	1.50	7
Cross-sectional area MCL (mm^2)	Wild-type	0.058^{+}	0.008	8
	TNX knockout	0.052	0.010	5

the laxity of the tail ligaments of the –/– mice was such to permit tying a knot in the tail; this is not possible in wild-type mice but has been described for the thrombospondin-2 knockout mouse (Kyriakides et al. 1998). We found, however, that this manipulation was not possible in the $TNX^{-/-}$ mouse (not shown). Secondly, as a measure for joint hypermobility, the stiffness of the MCL in the knee joint was analyzed. As shown in Table 2, our measurements did not reveal a difference in ligament stiffness between TNX knockout mice and wild-type littermates. In order to exclude the possibility of a thicker MCL in TNX knockout mice as a compensatory mechanism, we measured the mean thickness of the ligament by optical coherence tomography. The MCL thickness in TNX knockout mice did not significantly differ from wild-type littermates (Table 2). Histological analysis of wild-type and TNX knockout ligaments revealed no obvious differences (data not shown).

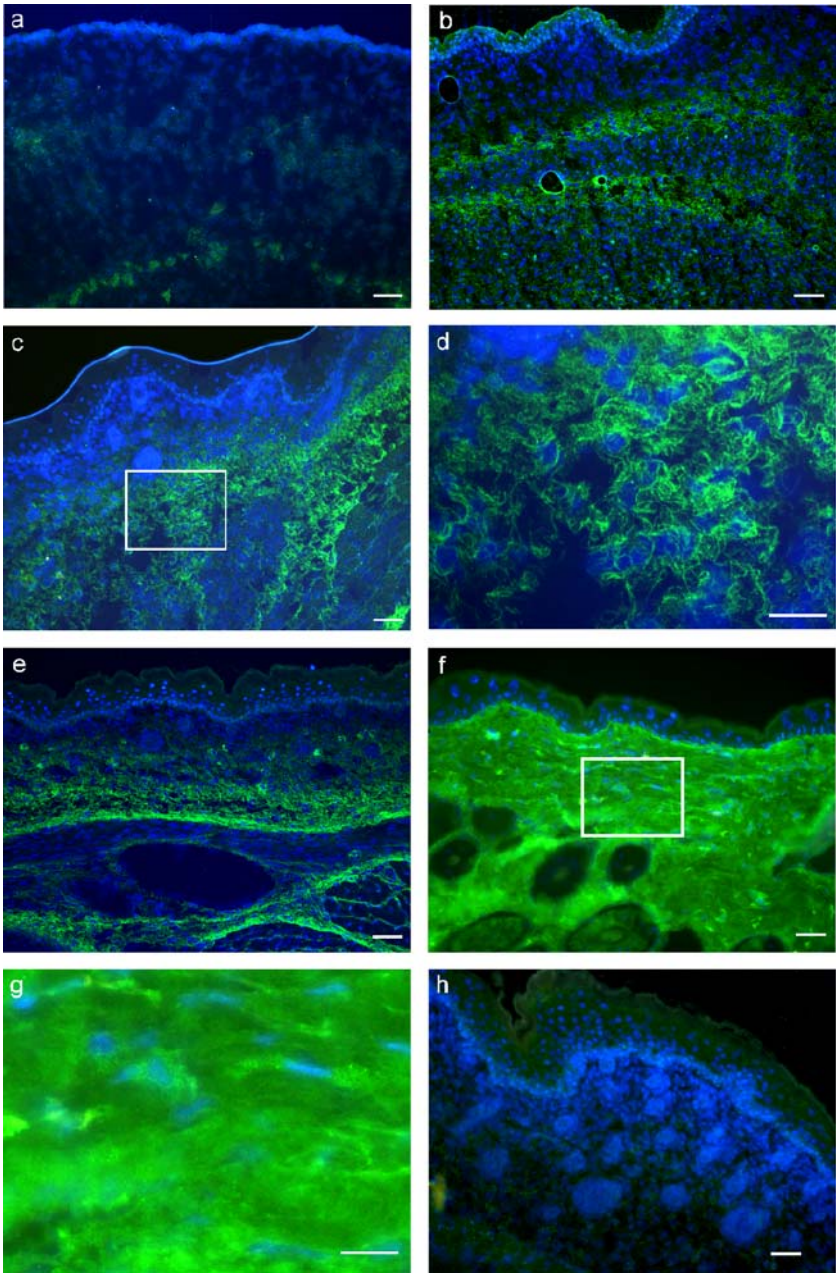

Fig. 2 TNX immunofluorescent staining of the developing skin of wild-type mice. **a** At stage E14, no significant signal in the prospective dermis is detected (*blue* nuclear staining with DAPI). **b** By stage E15, TNX expression (*green*) is visible in the developing reticular dermis and around the fascia of the carnosus muscle layer. **c**, **e** At E18 and in 1-day-old neonatal mice, respectively, expression of TNX has extended further into the dermis. **d** Higher magnification of the *rectangle* in **c**; TNX is expressed in the fetal mouse in a distinct fibre-like pattern. **f** In adult mouse skin, TNX is observed throughout the dermis in a more homogeneous pattern. **g** Higher magnification of the *rectangle* in **f**. **h** The specificity of the anti-TNX serum is demonstrated in TNX knockout mice skin (E18), which is devoid of signal. *Bars* 50 μm (**a**–**c**, **e**, **f**, **h**), 25 μm (**d**, **g**)

Expression of TNX in fetal and adult mouse skin

Sections of fetal, viz., embryonic day 13–20 (E13–E20), and adult skin were immunostained to reveal the expression of TNX at various developmental stages. The epidermis was devoid of signal at all stages, except for occasional non-specific staining of the stratum corneum. At E14, no significant signal was detected in the prospective dermis (Fig. 2a). From stage E15 onward, TNX expression was found in the lower dermis and around the fascia surrounding the panniculus carnosus beneath the developing dermis (Fig. 2b). TNX expression extended toward the

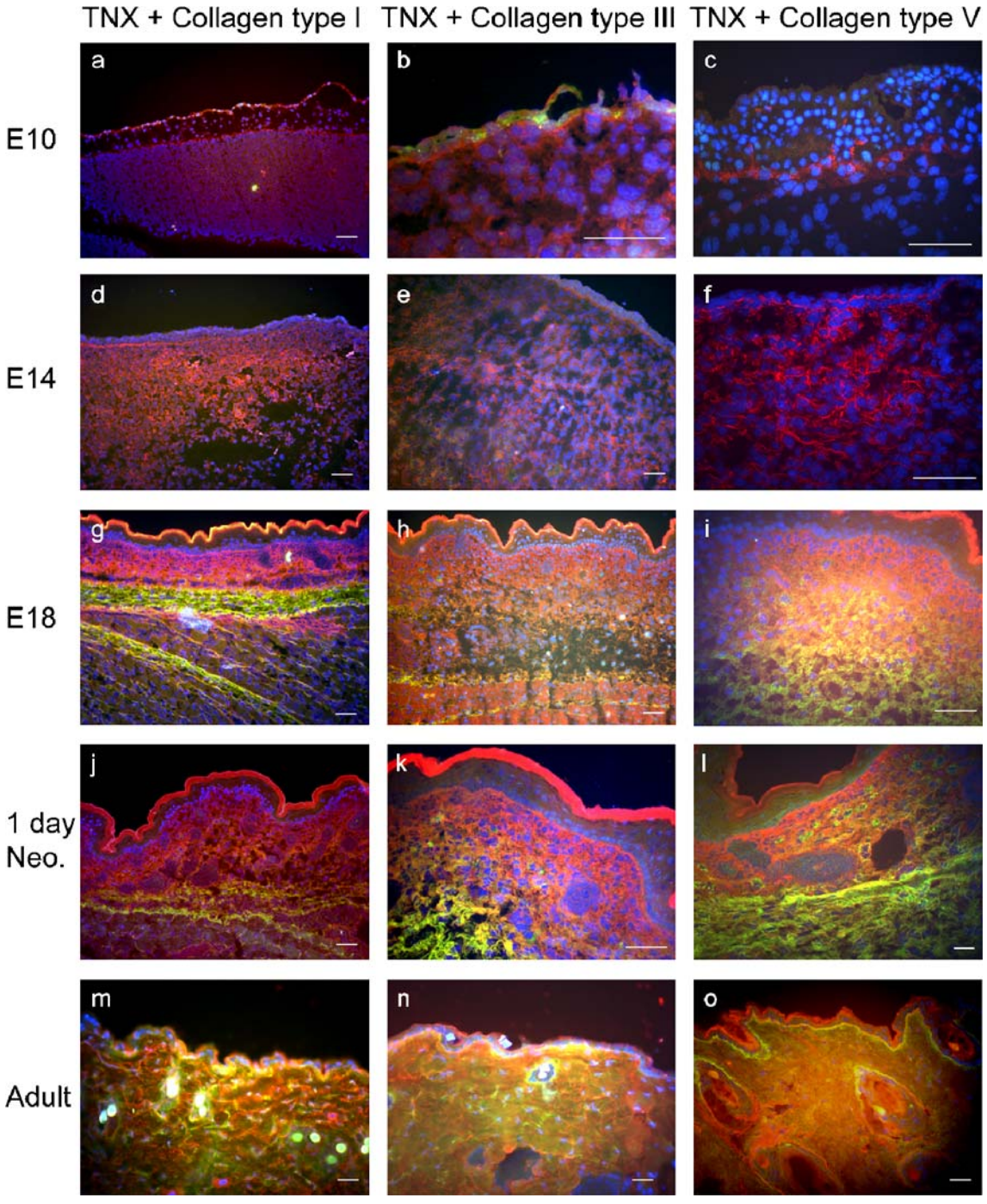

Fig. 3 Merged micrographs showing immunofluorescent double-staining for TNX (*green*) and collagens (*red*) type I (**a**, **d**, **g**, **j**, **m**), III (**b**, **e**, **h**, **k**, **n**), or V (**c**, **f**, **i**, **l**, **o**) in developing skin of wild-type mice. Nuclei are stained *blue* with DAPI. The different types of collagen are expressed even at fetal stages E10 (**a–c**) and E14 (**d–f**) in the prospective dermis. At E18 (**g–i**) and 1-day-old neonatal (*1 day Neo.*) mice (**j–l**), TNX starts to colocalize with the various types of collagens (*orange*, *yellow*). In adult mice, TNX is expressed in the entire dermis and overlaps with collagens type I (**m**), III (**n**), and V (**o**). Non-specific staining of the stratum corneum was present in some sections. *Bars* 50 μm

Table 3 Hydroxyproline (*OHP*) content in skin of adult (8–9 months old) mice as a measure for total collagen (^{+}P=0.09, ^{++}P=0.07)

Amount OHP	Genotype	Mean	SD	*n*
Content in nmol per mg protein	Wild-type	281.4^{+}	42.7	7
	TNX knockout	253.8	38.9	10
Content in nmol per mm^2 skin	Wild-type	31.6^{++}	10.4	7
	TNX knockout	24.7	8.3	10

upper part of the developing dermis at E18 and neonatal stages (Fig. 2c,e) and appeared in a fibre-like pattern (E18, Fig. 2d). In the adult mouse (Fig. 2f), the distinct fibre-like pattern was less clear, and the entire dermis exhibited a strong diffuse pattern (Fig. 2g). The specifity of our anti-TNX serum is illustrated in Fig. 2h, which shows the complete absence of staining at the E18 stage of a TNX knockout mice.

Differences in spatio-temporal appearance of TNX and the dermal fibrillar collagens

To address the question of whether TNX is involved in the assembly of collagen fibrils during normal dermal differentiation, we examined the appearance of collagens type I, III, and V in comparison with TNX. Collagens type I, III, and V were weakly present on E10 (Fig. 3a–c) in the undifferentiated dermal mesenchyme beneath the periderm of normal mouse fetuses (red signal). Expression of these collagens was abundant at E14 (Fig. 3d–f) before the start of TNX expression. The fibre-associated expression pattern of TNX, however, overlapped with the collagen network in the reticular dermis (orange signal) and around the fascia of the panniculus carnosus (orange and yellow signals), as shown in the overlays of the immunofluorescent stainings from E18 and 1-day-old neonatal mice (Fig. 3g–l). In the papillary dermis, the various collagen types were stained red, and TNX expression had not yet started in this compartment (Fig. 3g–l). In adult mice, TNX was expressed diffusely throughout the dermis and overlapped with collagens type I, III, and V, which were also expressed throughout the dermis (orange and yellow signals; Fig. 3m–o). No obvious differences in expression of the various collagen types and TNX were noted between TNX knockout and wild-type mice during development (data not shown).

Previous studies in mouse and human have shown that collagen content is reduced in adult skin of TNX-deficient individuals (Mao et al. 2002; Schalkwijk et al. 2001). Because immunofluorescent staining of dermal collagens could not be used to quantify collagen content, we performed an analysis of OHP content in TNX knockout and wild-type mouse skin. We found a slight reduction in collagen content, but this was not as prominent as in previous studies (Table 3).

Differences in spatio-temporal appearance of TNX and elastin

To address the question of whether TNX is involved in the assembly of elastic fibers during dermal differentiation, we used an antibody directed against TE as a marker for developing elastic fibers. A thin discontinuous layer of TE expression was present even in the undifferentiated dermal mesenchyme at E10 (red staining in Fig. 4a). Thereafter, TE staining was strong and continuous in the fascia lining the developing muscle cells of the panniculus carnosus. At E18, many TE-positive fibers were found in the outer layer of the fascia and scattered throughout the prospective reticular dermis as witnessed by the orange-yellow staining in merged double-staining images (Fig. 4b). Clearly, TNX expression differed temporally and spatially from TE expression in the developing mouse skin. However, from E15 onward, TNX started partially to colocalize with elastin. The TNX fibre-like pattern found at this stage overlapped with the pattern of TE-positive fibers around the fascia of the panniculus carnosus and in the prospective reticular dermis (Fig. 4b). In adult mouse skin, TNX was present diffusely throughout the entire dermis and therefore by definition overlaps with TE staining (Fig. 4c).

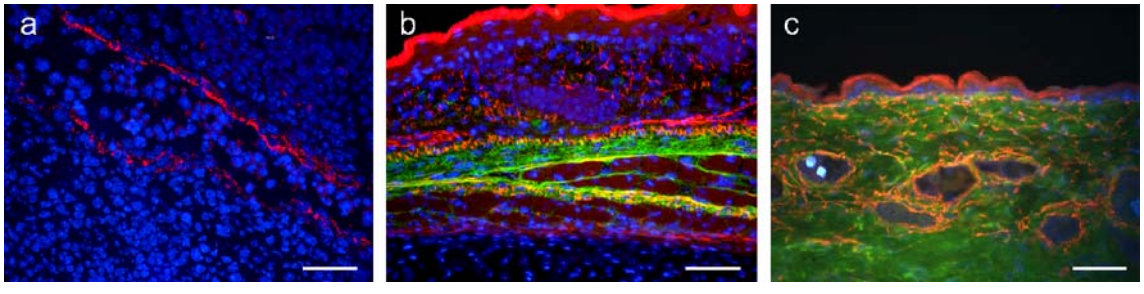

Fig. 4 Merged micrographs of immunofluorescent double-staining for TNX (*green*) and tropoelastin (TE; *red*) in developing skin in wild-type mice. TE is expressed in the undifferentiated mesenchyme at the earliest investigated stage, E10 (**a**). The signals for TE and TNX partially overlap (*orange*, *yellow*) in the developing mice skin around the fascia of the carnosus muscle at E18 (**b**). In adult mice (**c**), the entire dermis is stained positively for TNX with overlapping signal for TE (*orange*, *yellow*). *Bars* 50 μm

Difference in TE expression in knockout mice compared with heterozygous and wild-type mice

In adult TNX-deficient EDS patients, we have previously observed the fragmentation and clumping of elastic fibers (Zweers et al. 2004). We therefore examined the appearance of elastic fibers in adult knockout mice compared with heterozygous and wild-type mice by using immunofluorescent staining for TE. We did not observe obvious differences in the morphology or spatial distribution of the TE-positive elastic fibers, although the difference in density of the fibers was appreciable between adult wild-type and TNX knockout mice. Image analysis followed by computational quantitation showed that the signal intensity for TE was significantly higher in TNX knockout (Fig. 5c) mice than in heterozygous (Fig. 5b) and wild-type (Fig. 5a) littermates. The difference in density appeared at 3–6 months of age (Fig. 5e). Wild-type and heterozygous mice did not significantly differ in signal intensity. We subsequently investigated whether the differences in density of TE-positive fibers were reflected in the density of mature elastic fibers as determined histochemically by

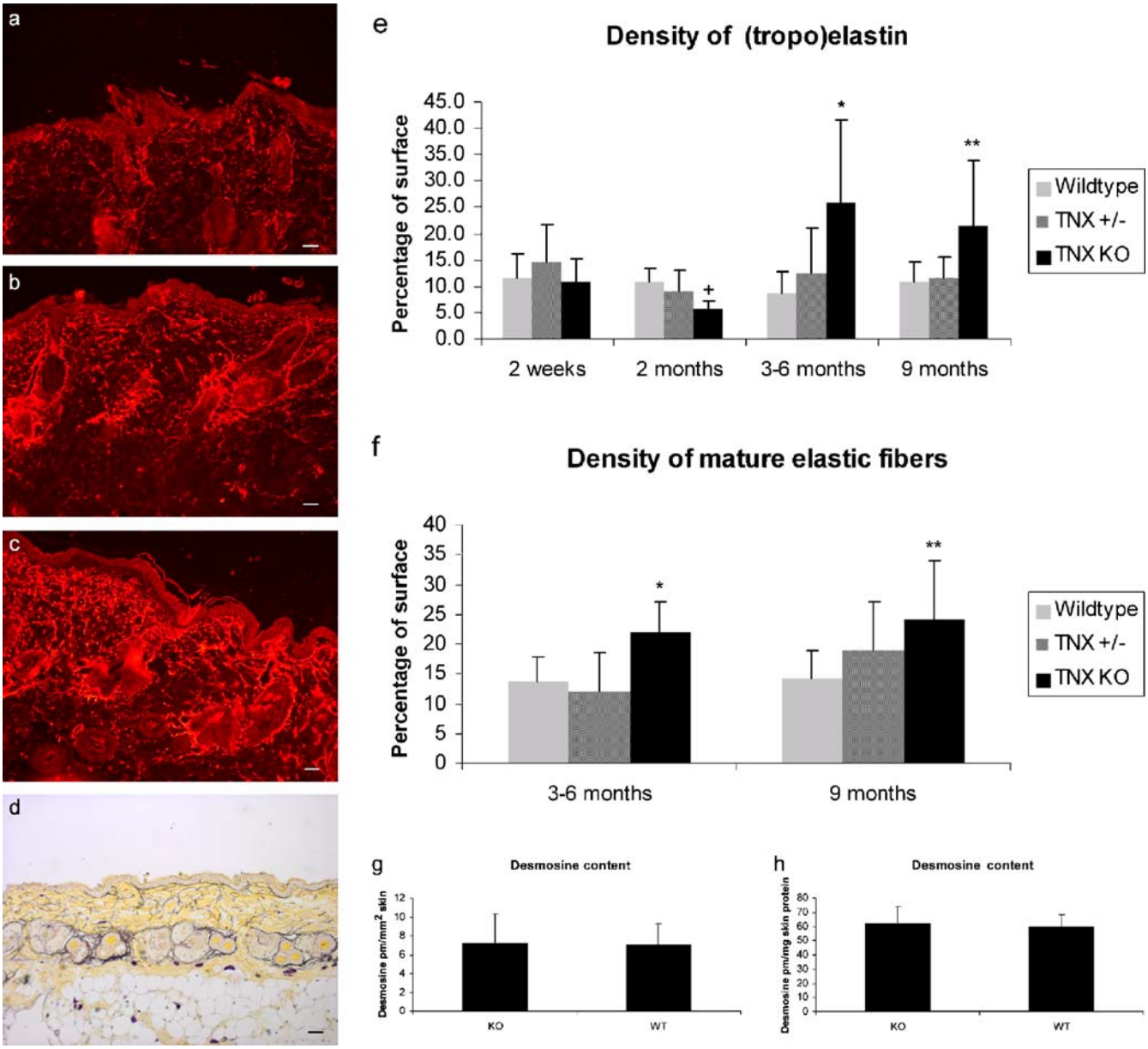

Fig. 5 Analysis of elastin and elastic fibers. Immunostaining for TE on paraffin sections of 9-month-old mice (**a**–**c**). At 3–6 months, TNX knockout mice (**c**) show a higher density of TE in their dermis than do wild-type (**a**) and heterozygous (**b**) mice (represented graphically in **e**). The density of mature elastic fibers made visible by modified Hart's staining in TNX knockout skin (not shown) compared with wild-type mice (**d**) is increased (**f**). No differences in desmosine content expressed per milligram protein (**h**) or per mm^2 (**g**) skin were found between the different phenotypes in adult mice. *P<0.01, **P<0.05, + not significant. For all comparisons, n=12 for each genotype for mice at 3–6 months, n=6 (or more) for mice at 2 weeks and 9 months. For 2-month-old mice, n=8 for heterozygous mice, n=4 for TNX knockout mice and n=3 for wild-type mice (*KO* knockout, *WT* wild-type, +/− heterozygous)

modified Hart's staining (shown for wild-type in Fig. 5d). Although the differences between wild-type and TNX knockout mice were not as obvious as for the TE immunostaining, computational analysis showed a significant difference in the densities of mature elastic fibers between TNX knockout and wild-type mice (Fig. 5f). To investigate these differences between wild-type and knockout mice further, we measured the amount of desmosine, a tetrafunctional crosslink specific for elastin, in mouse skin. Desmosine content did not differ between wild-type and knockout mice, irrespective of whether it was expressed per milligram protein or per skin surface area (Fig. 5g,h).

Discussion

The aim of our investigations was to provide a detailed study of TNX expression in skin and to examine the consequences of TNX deficiency at the functional and morphological levels. We have found no obvious differences in tail mobility and MCL stiffness, which we have used as a measure for joint hypermobility, between wild-type and knockout mice. We conclude that TNX knockout mice show a similar skin phenotype as human TNX-deficient patients but that these mice are not a suitable model to investigate joint hypermobility. On the basis of colocalization studies, we surmise that TNX is more likely to be involved in the maturation and maintenance of the collagen and elastin network than in its initial deposition.

TNX expression has not yet been studied in depth during the development of the skin. Geffrotin et al. (1995) have reported TNX transcripts in 87-day-old pig fetuses. Matsumoto et al. (1994) have demonstrated TNX transcripts in mice at E17 and staining of the dermis, but this is less strong toward the dermis at E15.5. This is in accordance with our data. However, no data from other fetal stages have been published, and TNX expression has not been studied at the protein level. We show that expression starts at E15 and progresses from the reticular dermis toward the papillary dermis during development. TNX is expressed in a fiber-like network during development, but this network is lost in adulthood. This suggests a possible difference in function for TNX during the development of skin and in mature skin.

We suggest that TNX is not involved in the initial deposition of collagen fibrils or elastic fibers because expression of the dermal fibrillar collagens and expression of TE starts well before TNX is expressed in the dermis. However, during development, the characteristic fiber-like pattern of TNX colocalizes with the collagens type I, III, and V networks; this is in accordance with previously results showing that TNX colocalizes with banded collagen fibrils in bovine fetal skin (Lethias et al. 1996; Elefteriou et al. 1997). The expression of the various types of fibrillar collagens in developing mouse skin has not been comprehensively studied in detail at the protein level. Van Exan and Hardy (1984) have found that fibrils are present at the earliest of investigated fetal stages (E12), and Niederreither et al. (1995) have demonstrated, by using in situ hybridization, that collagens type I and III are expressed in dermatomes at E10.5 and E12.5 in the presumptive dermis of whole mouse fetuses. The expression of collagen type V appears to mimic that of collagen type I, and transcripts are localized to dermal cells (Garrone et al. 1997; Andrikopoulos et al. 1992). These data are in accordance with our findings at the protein level.

A reduction in collagen occurs in the skin of adult TNX knockout mice (Mao et al. 2002) similar to that in TNX-deficient patients (Zweers et al. 2004). Although we have found a small difference in OHP content between TNX knockout and wild-type mice, the differences are not as profound as observed by Mao et al. (2002). Of note, the TNX null allele used in our study is on a different (homogenous C57Black6) background than that used by Mao et al. (2002). Together with the reduction of collagen, Mao et al. (2002) have found a decrease in the stress-strain properties of adult TNX knockout mice. We have confirmed this alteration of skin biomechanical properties in a test of skin breaking strength. We have found that, even at the youngest possible investigated age (2-week-old mice), skin strength is severely disturbed. Although no gross abnormalities of the collagen fibrils have been observed, a minor increase in size variation has been reported (Mao et al. 2002). Moreover, Minamitani et al. (2004) have found an increase in thickness of collagen fibrils in 3-month-old mice. Differences in skin mechanical properties between wild-type and TNX knockout are probably not solely caused by differences in the collagen density of the skin; qualitative differences in, for example, crosslinking and interaction between collagen fibrils might also play a role.

In TNX-deficient patients, we have previously observed altered elastic fibers in sections stained by Elastica von Gieson stain (Zweers et al. 2004). This stain appears ill-suited for the visualization of fetal and neonatal elastic fibers in mice. We have instead used a TE antibody, which recognizes both soluble TE and cross-linked elastin. In addition, we have used modified Hart's stain, a histochemical stain suitable for the visualization of elastic fibers in mouse skin. Immunofluorescence on paraffin sections has revealed an increased density of TE/elastin in TNX knockout mice compared with heterozygous TNX and wild-type mice at 3–6 months of age. This difference in density for TE/elastin is reflected, although less prominently, in mature elastic fibers in the dermis detected by modified Hart's staining. The quantification of desmosine content, however, has revealed no significant differences, suggesting a lower amount of desmosine crosslinks per elastic fiber in TNX knockout mice, which might possibly lead to less stable elastic fibers. This could in turn lead to increased synthesis as a possible compensatory mechanism. The elastic fibers of the TNX knockout mice might also be more susceptible to breakdown, since the differences in TE/elastin density appear in adulthood, in which case the TE/elastin might pick up elastin breakdown products from elastic fibers. Once again, the TNX knockout mice might compensate for this by (over) producing new elastic fibers, but this awaits further investigation. The elastic fiber phenotype in the TNX knockout mice does not resemble the phenotype found in humans. The organization and cellular source of elastic fibers in mice is known to

differ from those in humans (Starcher et al. 1999, 2005). Both in humans and in mice, TNX appears to be involved in the maintenance of normal elastic fibers. However, TNX does not seem to be associated with the initial deposition of TE/elastin, as immureactivity to the TE antibody is detected in the dermis before TNX expression starts. TNX could nevertheless be involved in the maturation of elastic fibers, since mature elastic fibers only start to appear approximately 5 days post partum in mice, coinciding with the start of hair growth (Starcher et al. 2005).

The morphological and biochemical abnormalities in TNX-deficient skin are mild compared with the strongly disturbed biomechanical properties. This suggests that TNX exerts more subtle functions that contribute to connective tissue stability. Studies by others have previously indicated that TNX interacts with various other matrix molecules (Elefteriou et al. 1997, 1999, 2001; Ikuta et al. 2000; Lethias et al. 2001; Matsumoto et al. 1994; Minamitani et al. 2004). Obviously, the biomechanical properties of the matrix will be affected by these interactions, and this is clearly an area of future research.

Acknowledgements The authors acknowledge the assistance of Dirk J. Faber and Ton G. van Leeuwen of the Laser Center at the Academic Medical Center, Amsterdam, with the optical coherence tomography measurements.

References

Andrikopoulos K, Suzuki HR, Solursh M, Ramirez F (1992) Localization of pro-alpha 2(V) collagen transcripts in the tissues of the developing mouse embryo. Dev Dyn 195:113–120

Bristow J, Tee MK, Gitelman SE, Mellon SH, Miller WL (1993) Tenascin-X: a novel extracellular matrix protein encoded by the human XB gene overlapping P450c21B. J Cell Biol 122:265–278

Burch GH, Gong Y, Liu W, Dettman RW, Curry CJ, Smith L, Miller WL, Bristow J (1997) Tenascin-X deficiency is associated with Ehlers–Danlos syndrome. Nat Genet 17:104–108

Elefteriou F, Exposito J, Garrone R, Lethias C (2001) Binding of tenascin-X to decorin. FEBS Lett 495:44–47

Elefteriou F, Exposito JY, Garrone R, Lethias C (1997) Characterization of the bovine tenascin-X. J Biol Chem 272:22866–22874

Elefteriou F, Exposito JY, Garrone R, Lethias C (1999) Cell adhesion to tenascin-X mapping of cell adhesion sites and identification of integrin receptors. Eur J Biochem 263:840–848

Exan RJ van, Hardy MH (1984) The differentiation of the dermis in the laboratory mouse. Am J Anat 169:149–164

Garrone R, Lethias C, LeGuellec D (1997) Distribution of minor collagens during skin development. Microsc Res Tech 38:407–412

Geffrotin C, Garrido JJ, Tremet L, Vaiman M (1995) Distinct tissue distribution in pigs of tenascin-X and tenascin-C transcripts. Eur J Biochem 231:83–92

Geffrotin C, Horak V, Crechet F, Tricaud Y, Lethias C, Vincent-Naulleau S, Vielh P (2000) Opposite regulation of tenascin-C and tenascin-X in MeLiM swine heritable cutaneous malignant melanoma. Biochim Biophys Acta 1524:196–202

Gijssen Y, Sierevelt I, Kooloos J, Blankevoort L (2004) Stiffness of the healing medial collateral ligament of the mouse. Connect Tissue Res 45:190–195

Huang D, Swanson EA, Lin CP, Schuman JS, Stinson WG, Chang W, Hee MR, Flotte T, Gregory K, Puliafito CA, Fujimoto JG (1991) Optical coherence tomography. Science 254:1178–1181

Ikuta T, Ariga H, Matsumoto K (2000) Extracellular matrix tenascin-X in combination with vascular endothelial growth factor B enhances endothelial cell proliferation. Genes Cells 5:913–927

Ikuta T, Sogawa N, Ariga H, Ikemura T, Matsumoto K (1998) Structural analysis of mouse tenascin-X: evolutionary aspects of reduplication of FNIII repeats in the tenascin gene family. Gene 217:1–13

Kyriakides TR, Zhu YH, Smith LT, Bain SD, Yang Z, Lin MT, Danielson KG, Iozzo RV, LaMarca M, McKinney CE, Ginns EI, Bornstein P (1998) Mice that lack thrombospondin 2 display connective tissue abnormalities that are associated with disordered collagen fibrillogenesis, an increased vascular density, and a bleeding diathesis. J Cell Biol 140:419–430

Lethias C, Descollonges Y, Boutillon MM, Garrone R (1996) Flexilin: a new extracellular matrix glycoprotein localized on collagen fibrils. Matrix Biol 15:11–19

Lethias C, Elefteriou F, Parsiegla G, Exposito JY, Garrone R (2001) Identification and characterization of a conformational heparin-binding site involving two fibronectin type iii modules of bovine tenascin-X. J Biol Chem 276:16432–16438

Lindor NM, Bristow J (2005) Tenascin-X deficiency in autosomal recessive Ehlers–Danlos syndrome. Am J Med Genet A 135:75–80

Mao JR, Taylor G, Dean WB, Wagner DR, Afzal V, Lotz JC, Rubin EM, Bristow J (2002) Tenascin-X deficiency mimics Ehlers–Danlos syndrome in mice through alteration of collagen deposition. Nat Genet 30:421–425

Martin SD, Patel NA, Adams SB, Roberts MJ, Plummer S, Stamper DL, Brezinski ME, Fujimoto JG (2003) New technology for assessing microstructural components of tendons and ligaments. Int Orthop 27:184–189

Matsumoto K, Saga Y, Ikemura T, Sakakura T, Chiquet ER (1994) The distribution of tenascin-X is distinct and often reciprocal to that of tenascin-C. J Cell Biol 125:483–493

Matsumoto K, Takayama N, Ohnishi J, Ohnishi E, Shirayoshi Y, Nakatsuji N, Ariga H (2001) Tumour invasion and metastasis are promoted in mice deficient in tenascin-X. Genes Cells 6:1101–1111

Matsumoto K, Takahashi K, Yoshiki A, Kusakabe M, Ariga H (2002) Invasion of melanoma in double knockout mice lacking tenascin-X and tenascin-C. Jpn J Cancer Res 93:968–975

Matsumoto K, Minamitani T, Orba Y, Sato M, Sawa H, Ariga H (2004a) Induction of matrix metalloproteinase-2 by tenascin-X deficiency is mediated through the c-Jun N-terminal kinase and protein tyrosine kinase phosphorylation pathway. Exp Cell Res 297:404–414

Matsumoto K, Sato T, Oka S, Inokuchi J, Ariga H (2004b) Comparison of the compositions of phospholipid-associated fatty acids in wild-type and extracellular matrix tenascin-X-deficient mice. Biol Pharm Bull 27:1447–1450

Matsumoto K, Sato T, Oka S, Orba Y, Sawa H, Kabayama K, Inokuchi J, Ariga H (2004c) Triglyceride accumulation and altered composition of triglyceride-associated fatty acids in the skin of tenascin-X-deficient mice. Genes Cells 9:737–748

Minamitani T, Ikuta T, Saito Y, Takebe G, Sato M, Sawa H, Nishimura T, Nakamura F, Takahashi K, Ariga H, Matsumoto K (2004) Modulation of collagen fibrillogenesis by tenascin-X and type VI collagen. Exp Cell Res 298:305–315

Niederreither K, DSouza R, Metsaranta M, Eberspaecher H, Toman PD, Vuorio E, DeCrombrugghe B (1995) Coordinate patterns of expression of type I and III collagens during mouse development. Matrix Biol 14:705–713

Peeters ACTM, Kucharekova M, Timmermans J, Berkmortel FWPJ van den, Boers GH, Novakova IRO, Egging D, Heijer M den, Schalkwijk J (2004) A clinical and cardiovascular survey of Ehlers–Danlos syndrome patients with complete deficiency of tenascin-X. Neth J Med 62:23–25

Schalkwijk J, Zweers MC, Steijlen PM, Dean WB, Taylor G, Van Vlijmen IM, Haren B van, Miller WL, Bristow J (2001) A recessive form of the Ehlers–Danlos syndrome caused by tenascin-X deficiency. N Engl J Med 345:1167–1175

Starcher B (2001) A ninhydrin-based assay to quantitate the total protein content of tissue samples. Anal Biochem 292:125–129
Starcher B, Conrad M (1995) A role for neutrophil elastase in the progression of solar elastosis. Connect Tissue Res 31:133–140
Starcher B, Pierce R, Hinek A (1999) UVB irradiation stimulates deposition of new elastic fibers by modified epithelial cells surrounding the hair follicles and sebaceous glands in mice. J Invest Dermatol 112:450–455
Starcher B, Aycock RL, Hill CH (2005) Multiple roles for elastic fibers in the skin. J Histochem Cytochem 53:431–443
Waard JWD de, Wobbes T, Deman BM, Linden CJ van der, Hendriks T (1995) Postoperative levamisole may compromise early healing of experimental intestinal anastomoses. Br J Cancer 72:456–460
Zweers MC, Bristow J, Steijlen PM, Dean WB, Hamel BC, Otero M, Kucharekova M, Boezeman JB, Schalkwijk J (2003) Haploinsufficiency of TNXB is associated with hypermobility type of Ehlers–Danlos syndrome. Am J Hum Genet 73:214–217
Zweers MC, Vlijmen–Willems IM, Van Kuppevelt TH, Mecham RP, Steijlen PM, Bristow J, Schalkwijk J (2004) Deficiency of tenascin-X causes abnormalities in dermal elastic fiber morphology. J Invest Dermatol 122:885–891
Zweers MC, Peeters ACTM, Graafsma S, Kranendonk S, Vliet JA van der, Heijer M den, Schalkwijk J (2005) A high tenascin-X serum concentration is a risk indicator for abdominal aortic aneurysm. Circulation (in press)